ADVANCED MATERIALS TECHNOLOGIES
www.advmattechnol.de

Transparent, Sprayable Plastic Films for Luminescent Down-Shifted-Assisted Plant Growth

Rosa Müller, Bibian Okokhere-Edeghoghon, Norbert J. Janowicz, Andrew D. Bond, Gabriele Kociok-Kohn, Lynne M. Roxbee Cox, Diana Garzon, Toby W. Waine, Ian G. Truckell, Ewan Gage, Andrew J. Thompson, Dmitry Busko, Ian A. Howard, Monica S. Saavedra, Bryce S. Richards, Boris Breiner, Petra Cameron,* and Dominic S. Wright**

The world's steadily growing population and global heating due to climate change are a threat to food security. To meet this challenge, novel technologies are needed to increase crop production in a sustainable way. In this work, the use of luminescent down-shifting (LDS) materials based on molecular Eu^{3+}-containing polyoxotitanates for plant growth enhancement is investigated. Using a systematic design strategy to optimize down-shifting properties, conversion of the ultraviolet spectral range to the photosynthetically active radiation (PAR) is achieved with quantum yields as high as 68%. The prototype Eu^{3+}-compound can be incorporated into water-based acrylic varnish that can be spray-coated onto existing greenhouses. Comparing coated with uncoated greenhouses, basil plants produce 9% more leaf dry weight per plant, and a highly significant 10% increase in individual leaf dry weight. The coating reduces the amount of transmitted PAR by 8% but has advantageous effects on diffuse radiation and in reducing the internal mean temperature. Although there is some uncertainty as to the contribution of down-shifting, with the bulk of the increase probably being due to higher diffused light and the reduction in maximum daily temperatures, this study establishes a model for the design of LDS paints for real-world agricultural applications.

1. Introduction

The dramatic climatic effects of global warming, with the increasing potential for chaotic weather conditions and extremes of temperature, are likely to have far-reaching effects on the ability to preserve habitat or even to sustain life in various regions of the planet. One of the most important conclusions of the 2015 Paris Agreement on climate change is that even with more efficient use of fossil fuels, and the resulting reduction in carbon emissions, it will be impossible to keep the average rise in global temperature to below safe targets without significant scientific innovations.[1] While the governmental policies at large have been focused on renewable energy as a means of offsetting the impending effects of global warming, there has been increasing alarm and public concerns over the way that climate

R. Müller, N. J. Janowicz, A. D. Bond, D. S. Wright
The Yusuf Hamied Chemistry Department
Cambridge University
Cambridge CB2 1EW, UK
E-mail: dsw1000@cam.ac.uk

B. Okokhere-Edeghoghon, G. Kociok-Kohn, P. Cameron
Department of Chemistry
1 South University of Bath
Claverton Down, Bath BA2 7AY, UK
E-mail: p.j.cameron@bath.ac.uk

L. M. R. Cox, D. Garzon, T. W. Waine, I. G. Truckell, E. Gage, A. J. Thompson
School of Water, Energy and Environment
Cranfield University
Cranfield, Bedfordshire MK43 0AL, UK

D. Busko, I. A. Howard, B. S. Richards
Institute of Microstructure Technology
Karlsruhe Institute of Technology (KIT)
Hermann-von-Helmholtz-Platz 1, 76344 Eggenstein-Leopoldshafen, Germany

M. S. Saavedra, B. Breiner
Lambda Energy Ltd.
Crop Technology Southern Innovation Hub
College Road, Cranfield MK43 0AL, UK
E-mail: boris@lambda.energy

The ORCID identification number(s) for the author(s) of this article can be found under https://doi.org/10.1002/admt.202400977

DOI: 10.1002/admt.202400977

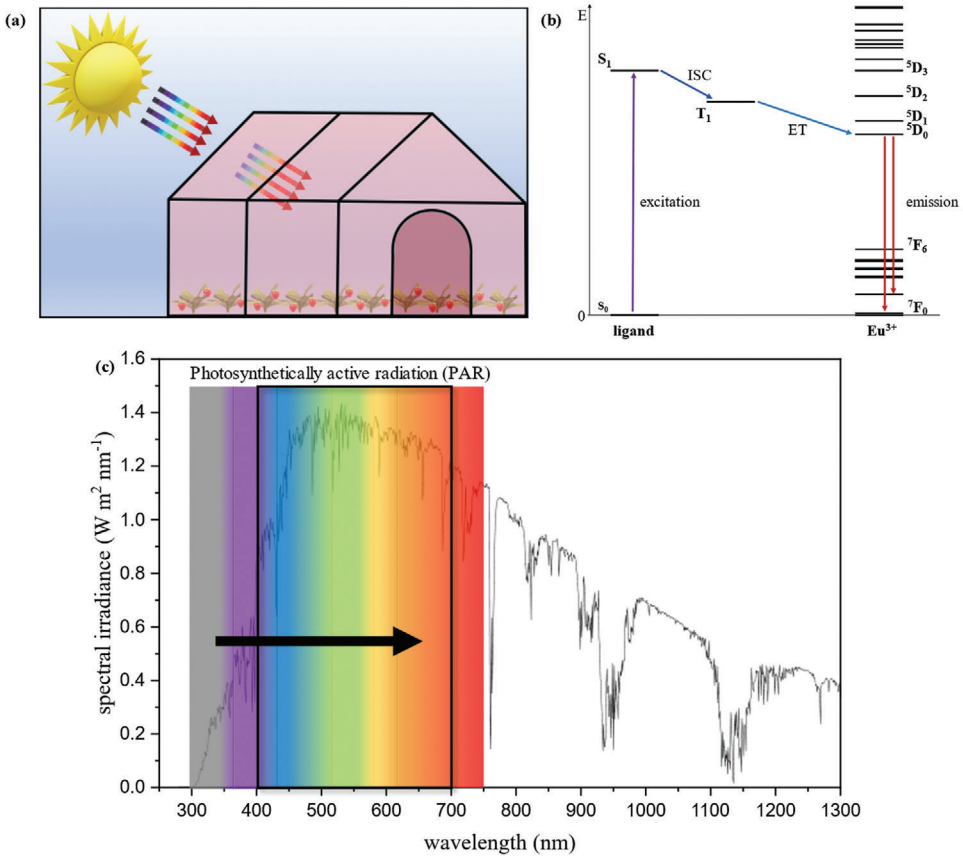

Figure 1. a) The concept of LDS assisted plant growth (illustrated using a molecular Eu^{3+}-based luminophore as the emissive material coated on a glass greenhouse). b) The luminescence mechanism involving HOMO-LUMO energy transfer (ET) of a light-harvesting (antenna) ligand via Intersystem Crossing (ISC) to a triplet intermediate (T_1) to the *4f* levels of Eu^{3+}. c) The air-mass 1.5 global solar spectrum (ASTM G173-03 Reference Spectrum) as measured at sea level on Earth showing the absorbed UV range (grey/violet), which is converted to red light as part of the PAR.

change will affect global food supplies, especially considering the increasing human population which is set to reach 9–10 billion by 2050.[2] This has been brought into sharper focus by recent geopolitical concerns, most obviously the invasion of Ukraine and its impact on the global supply of, among other important commodities, wheat and sunflower oil.[3] This interplay between energy and food extends to water – the so-called energy-water-food nexus – which lies at the heart of sustainable development, especially considering that the demand for all three vital resources is increasing rapidly.

Against the backdrop of more frequent weather extremes, rising human population and use of precious energy resources for food transport, it is not surprising that many nations are looking to become more self-sufficient in food production, where controlling costs and limiting energy use are especially important. Protected cropping, i.e., production of fresh produce such as tomatoes, cucumbers, peppers, leafy salads, and soft fruits, under glass or polyethylene, increases growing temperatures so that crops can be grown in extended seasons and with more optimal temperatures for higher yield (warming by "greenhouse effect" in the cooler seasons, and shading in the summer). Protected crops in temperate climates are often limited by light in the shorter days of spring and autumn due to low daily light integrals, hence supplementary lighting is often used to enhance growth, but this is becoming uneconomic due to escalating energy costs and net zero carbon emission goals. Indeed, it has been reported that electricity consumption comprises >10% of the sales from greenhouse products with lighting typically comprising 15–25% of that total.[4,5] One solution to this is to employ passive optical materials that can convert higher-energy photons from the solar spectrum into lower-energy light in the range of photosynthetically active radiation (PAR, defined as radiation between 400 and 700 nm). Not all wavelengths in this range are used with the same efficiency, and plants have complex photosynthetic responses to different combinations of PAR wavelengths, making spectral shifts within the PAR range also of potential interest.[6] It has been demonstrated that for most plant species ultraviolet photons in the UV-B (280–320 nm) and UV-A (320–400 nm) radiation range contribute little towards photosynthesis, whereas blue photons (400–500 nm) can have a controlling effect on the plant growth, which suggests an ideal conversion range from 400 nm to shorter wavelengths.[7] Such a process would add to the existing PAR and result in increased crop yields at a lower energy cost (**Figure 1a**). Developing technologies in this area rely on luminescent down-shifting (LDS) materials employing organic dyes (e.g., including specialized dyes developed by BASF in the 1980s for solar energy conversion) or more recently using quantum dots (specifically developed for agriculture)

as the emissive materials embedded in plastic films.[8–11] While organic dyes are cheap, readily available, and exhibit high photoluminescent quantum yields (PLQYs), they often suffer from photo-bleaching (photochemical degradation) which leads to limited lifetimes. Quantum dots can exhibit much longer lifetime, but are expensive, difficult to prepare at scale, and require surface modification to prevent quenching of the luminescence in the plastic matrix.[12] However, impressive increases in crop yields of ≈20% have been claimed by commercial companies using these technologies.[13]

An alternative to quantum dots or organic dyes are molecular luminophores containing trivalent lanthanide-ions such as Eu^{3+}, which absorb in the UV and emit in the desired red range of the visible spectrum. The luminescence mechanism is different from that of organic dyes or quantum dots, involving electronic relaxation from higher- to lower-energy *f*-states of the lanthanide ion. However, the absorption cross-section of *f-f* electronic transitions is very weak and the excited states have long lifetimes, which increases the probability of non-radiative decay or quenching. Therefore, this process leads to very low external PLQYs for isolated ions and normally an "antenna" (light-harvesting) ligand with matching energy levels is required to increase the absorption cross-section and efficiently populate the emissive states of the lanthanide (Figure 1b). In the first very recent study on this idea, it was reported that a dichloromethane solution of the coordination compound $[Eu(hfa)_3(TPPO)_2]$ (hfa = hexafluoroacetylacetonato, TPPO = triphenylphosphine oxide) can be painted onto polyolefin plastics to produce UV-to-red LDS materials, which resulted in the reported increases in plant height and dry-mass crop yields.[14] However, these plant studies had limited statistical significance, the lifetime and PLQY of the film are low (63 days and 26%, respectively), and the method is not applicable to glass coatings or to recoating in an agricultural setting.

Apart from being cheap, scalable, and robust, absorbing the desired part of the UV- and blue range of the solar spectrum (280–400 nm), and possessing high PLQYs, the ideal luminophores for large-scale food production would be highly compatible with a range of plastics, allowing the broadest range of applications in flexible plastic sheets, free-standing plastic panes or potentially in sprayable plastic coatings on glass. Since UV accounts for only 3–5% of ambient sunlight at sea level (in terms of photon flux), the ability to tune the antenna ligand to harvest additional blue light would be advantageous as this would significantly increase the amount of emitted red photons (600–700 nm). The design of robust molecular Eu^{3+}-based luminophores possessing in-built modularity to address these specifications is therefore an important starting point – specifically, having stable core structures which preserve molecular integrity (and PLQY) in plastic matrices, and allowing selective modification of the antenna and solubilizing ligands without inducing major structural changes (which might adversely affect photophysical properties).

In this paper, we develop an approach based on readily prepared and cheap Eu^{3+}-containing polyoxotitanium cages (Eu-POTs) which, we show, possess the necessary design features listed before. Having established the ground rules for selective modification, we introduce a working prototype luminophore with high PLQY (>60%) which is soluble in a range of commercial plastics, including water-based acrylic paint that can be sprayed onto conventional glass greenhouses in an agricultural environment. Using plant-growth experiments in domestic, acrylic-sprayed glass greenhouses (versus un-sprayed), we show a highly significant 10% increase in the individual leaf dry mass (i.e., grams per leaf) of basil, and a trend towards higher mass per plant. This study serves as a systematic model for the development of new, sprayable down-shifting greenhouse coatings in the real world.

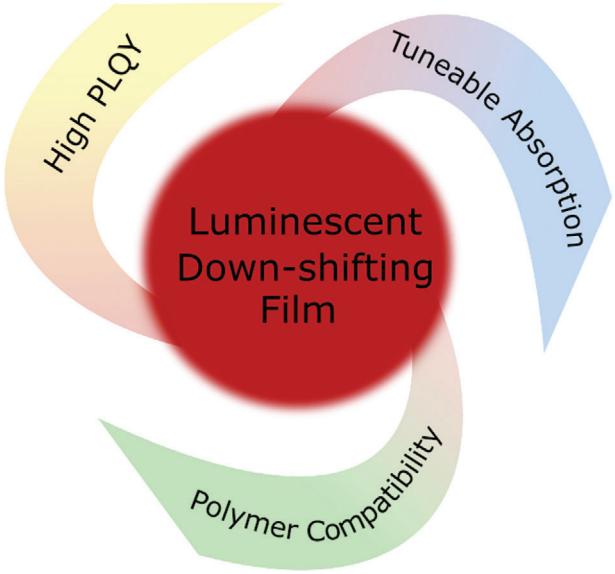

Scheme 1. The main design concept for targeting suitable Eu-POT for down-shifting applications.

2. Results and Discussion

2.1. Design Strategy

Molecular, europium-containing polyoxotitanium cages (Eu-POTs) appear to be good candidates as luminophores based on the previously discussed design criteria (outlined in **Scheme 1**). They possess potentially adaptable organic ligand peripheries to promote solubility in various media as well as rigid Eu^{3+} coordination environments, which are likely to ensure the maintenance of molecular structure and photophysical properties in plastic matrices. The key issues we addressed in our preliminary studies were (i) whether the ligand periphery of Eu-POTs can be changed without modifying the cage structure and coordination environment of the Eu^{3+} ion, and (ii) whether the incorporation of functional groups can be used to shift the absorption edge further into the visible region. For this purpose, we selected the previously reported Eu_8Ti_{10} cage $[Eu_8Ti_{10}(\mu_3\text{-}O)_{14}(tbba)_{34}(OAc)_2(H_2O)_4(THF)_2]$ (**1**, tbba = 4-*tert*-butylbenzoate, **Figure 2**) as a model system, based on the comparatively cheap synthetic components involved, its reported moisture/air stability and high PLQY (73% in the solid state).[15] Cage **1** was obtained using the literature procedure by the reaction of $Eu(OAc)_3$ with $Ti(O^iPr)_4$ and 4-*tert*-butylbenzoic acid (Htbba) in anhydrous acetonitrile/THF at 70 °C.

Cage **1** showed poor compatibility with a polymethylmethacrylate (PMMA) matrix, leading to poor film quality and low

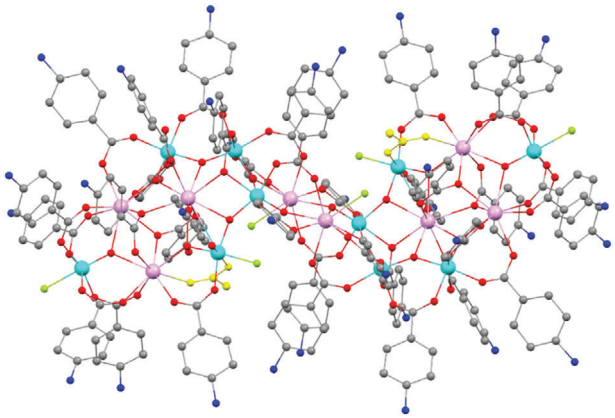

Figure 2. General structure of $[Eu_8Ti_{10}(\mu_3\text{-}O)_{14}(L)_{34}(OAc)_2(H_2O)_4(THF)_2]$-type POTs with the two acetate ligands shown in yellow and the H_2O/THF coordination sites in green. The functional groups at the para-positions of the benzoate ligands where ligand modification is involved in the current study are labeled in dark blue. The single-crystal data for L = 4-methoxybenzoate has been used in this figure. Hydrogen atoms were omitted for clarity. A consistent coloring scheme is used throughout this work: Ln = pink, Ti = light blue, C = grey, O = red, N = mid blue, F = green.

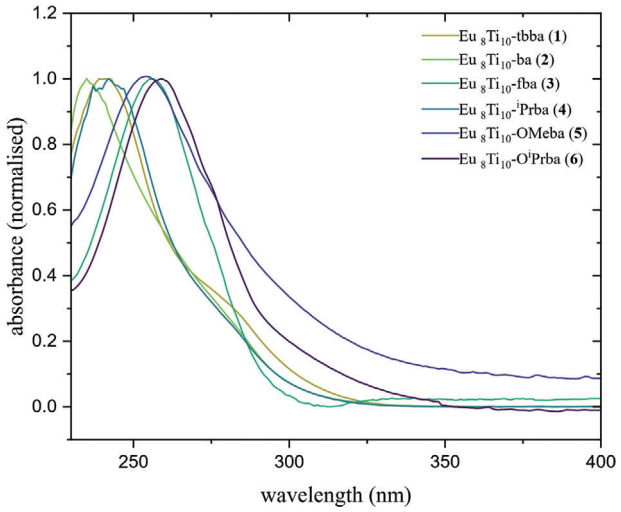

Figure 3. Normalized solution-state UV–vis absorption spectra of the Eu_8Ti_{10}-based compounds **1**–**6** (0.033 mg mL^{-1} in DCM). The absorption maxima were determined (in order of increasing absorption edge) as 235 nm (**2**), 239 nm (**1** and **4**), 254 nm (**5**), 256 nm (**3**) and 259 nm (**6**). The offset in the spectrum of compound **5** from 350 nm onward is a normalization artifact.

concentrations of active material (only up to 1 mg g^{-1}). Furthermore, despite the reported molecular PLQY of 73% (solid state) for **1**, our measurements indicate a much lower value of 22% for solid **1** and ≈28% in PMMA (1 mg/g).[15] Combined with an absorption onset at 310 nm, these optical properties are clearly insufficient for the promotion of plant growth as both the absorbed fraction of the solar spectrum and the efficiency of the LDS process are too low. Nonetheless, we were able to use compound **1** as a basis for tuning the absorption edge and solubility properties. By substituting only the para-positions of the benzoate ligands with various electron-donors and -acceptors, a series of new cages having the same Eu_8Ti_{10} core arrangement as **1** was obtained using a similar synthetic procedure: $[Eu_8Ti_{10}(\mu_3\text{-}O)_{14}(ba)_{34}(OAc)_2(H_2O)_6(MeCN)_2]$ (**2**, ba = benzoate), $[Eu_8Ti_{10}(\mu_3\text{-}O)_{14}(fba)_{34}(OAc)_2(H_2O)_6(MeCN)]$ (**3**, fba = 4-fluorobenzoate), $[Eu_8Ti_{10}(\mu_3\text{-}O)_{14}(^{i}Prba)_{34}(OAc)_2(H_2O)_4(THF)_2]$ (**4**, ^{i}Prba = 4-isopropylbenzoate), $[Eu_8Ti_{10}(\mu_3\text{-}O)_{14}(OMeba)_{34}(OAc)_2(H_2O)_6]$ (**5**, OMeba = 4-methoxybenzoate) and $[Eu_8Ti_{10}(\mu_3\text{-}O)_{14}(O^{i}Prba)_{34}(OAc)_2(H_2O)_4(THF)_2]$ (**6**, O^{i}Prba = 4-isopropoxybenzoate). All these compounds are isostructural with compound **1**, apart from slight differences in the ligand connectivity and solvent coordination, depending on the crystallization conditions. Analysis of the bond lengths and angles shows no significant variation across the series, which indicates that substitution at the 4-position of the phenyl rings has little structural impact. Furthermore, upon replacement of $Eu(OAc)_3$ with $Eu(met)_3$ (met = methacrylate) as a precursor in the synthesis, the new cage $[Eu_8Ti_{10}(\mu_3\text{-}O)_{14}(tbba)_{34}(met)_2(H_2O)_4(THF)_2]$ (**7**) was obtained, again having the same Eu_8Ti_{10} core arrangement and demonstrating that a variety of ligand modifications can be achieved without inducing major changes to the molecular structure.[16]

With bulk samples of the series of Eu_8Ti_{10} cages (**1**-**6**) in hand, we could assess the effects of ligand substitution independently of structural change. The UV-visible spectra of the complexes in DCM are shown in **Figure 3**.

A small bathochromic shift of 4 nm is observed for alkyl-substituents [^{i}Prba (**4**) and tbba (**1**)] compared to compound **2** (containing unsubstituted benzoate ligands). The introduction of oxygen-donor (^{i}PrO) groups in **6** increases the shift by a further 20 nm, having a slightly larger effect than that of MeO groups in **5** (17 nm). Compound **3** (fba) shows the most blue-shifted absorption onset within the series due to the electron-withdrawing character of the fluoride ligands but exhibits an absorption maximum within the range of the alkoxy-substituted cages **5** and **6**.

The PLQY values measured for compounds **1**–**6** (solution state) and for the polymethylmethacrylate film samples of **1** and **5** are summarized in **Table 1**. For compound **5** improved compatibility with the PMMA matrix was observed compared to **1**. In addition, full analysis of a test film of **5** showed improved absorption properties together with better overall film quality. Clearly, the PLQYs (**Φ**) of all the cages are too low to provide sufficient photon flux for plant growth, especially considering the high energy of their absorption edges (only in the UV region). Nonetheless, these pilot studies do show that ligand modification of a parent Eu-POT can be achieved without structural changes, that ligand modification can be used to improve compatibility with plastic matrices, and that electron-donating substituents can be used to promote favorable light-harvesting properties in Eu-POT cages. Furthermore, the long calculated radiative lifetime (τ_{rad}) indicates that despite the changes in the ligand periphery, the Eu^{3+} ion environments within the POTs are maintained in the plastic films, and that the rigid coordination environment protects the lanthanide ion from interaction with solvent molecules or the polymer matrix. This prevents fast deactivation and a loss of energy through non-radiative vibronic interactions.

Table 1. Summary of the quantum yield measurements for the Eu_8Ti_{10}-based compounds **1**–**6** and the corresponding PMMA film samples. The compounds were measured in solution (DCM) upon excitation at 300 nm, whereas the films were measured as solid-state samples. The concentrations of active material in the PMMA samples are 1 mg g^{-1} for **1** and 5 mg g^{-1} for **5**.

	Φ [%][a]	$\Phi_{intrinsic}$ [%]	τ_{rad} [ms][b]	τ_{exp} [ms]	$\Phi_{ligand\rightarrow Eu}$ [%][c]
1	22	51	2.4	1.2	43
2	26	44	2.5	1.2	59
3[d]	3.2	–	2.4	–	–
4	30	45	2.4	1.3	67
5	3.1	57	2.0	1.1	5.4
6	1.0	47	2.2	1.1	2.1
1 in PMMA	21	40	2.2	0.9	53
5 in PMMA	15	48	2.3	1.1	31

[a] For all absolute values an uncertainty of ≈±10% is assumed due to the high Stokes shift and low sensitivity of the system (including the corresponding corrections) in the UV range; [b] Obtained from sensitivity-corrected emission spectra as described in the literature[17]; [c] Calculated from $\Phi_{tot} = \Phi_{intrinsic} \times \Phi_{ligand\rightarrow Eu}$; [d] Not enough sample material was obtained to measure reproducible values.

Table 2. Summary of the quantum yield measurements for the Eu_2Ti_4-based compounds **8**–**13** and the corresponding PMMA film samples. The compounds were measured in solution (DCM) upon excitation at 300 nm, whereas the films were measured as solid-state samples with a concentration of active material of 1 mg g^{-1}.

	Φ [%][a]	$\Phi_{intrinsic}$ [%]	τ_{rad} [ms][b]	τ_{exp} [ms]	$\Phi_{ligand\rightarrow Eu}$ [%][c]
8	53	67	3.9	2.6	79
9	74	–	3.6	–	–
10	60	66	3.6	2.4	91
11	1.3	–	3.7	–	–
12	31	–	3.6	–	–
13	68	–	4.1	–	–
8 in PMMA	50	62	3.4	2.1	81
10 in PMMA	46	65	3.3	2.1	71
13 in PMMA	68	68	3.2	2.2	100

[a] For all absolute values an uncertainty of ≈±10% is assumed due to the high Stokes shift and low sensitivity of the system (including the corresponding corrections) in the UV range; [b] Obtained from sensitivity-corrected emission spectra as described in literature[17]; [c] Calculated from $\Phi_{tot} = \Phi_{intrinsic} \times \Phi_{ligand\rightarrow Eu}$.

2.2. Refining the Active Component

The absence of antenna ligands directly bonded to Eu^{3+} in **1**–**6** is an obvious reason for their low PLQYs. Consequently, we sought a more viable candidate Eu-POT framework which would allow us to overcome this hurdle. We selected the readily synthesized, air-stable cage $Eu_2Ti_4O_6(phen)_2(met)_{10}$ (met = methacrylate, phen = 1,10-phenanthroline) (**8**, **Figure 4**) as a prototype, in which the antenna ligand phenanthroline coordinates the Eu^{3+} centers directly.[18] This structural feature leads to more efficient sensitization and therefore higher quantum yields (reported as 75% in the solid state, and 56% in DCM). We were able to verify the reported quantum yield in solution (53% in DCM) and, importantly, we showed that this PLQY is maintained in a PMMA film (50% at 5 mg g^{-1} concentration) (**Table 2**). The latter strongly suggests (again) that the molecular units of **8** are maintained in the PMMA matrix.

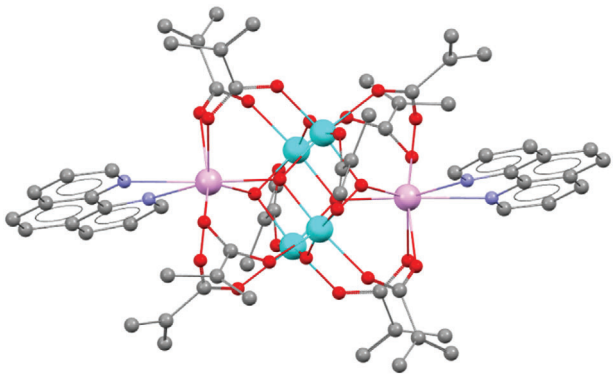

Figure 4. Single-crystal structure of $Eu_2Ti_4O_6(phen)_2(met)_{10}$ (**8**), showing the direct sensitization of the Eu^{3+}-centers with 1,10-phenanthroline. Hydrogen atoms were omitted for clarity. The structural data were obtained from the CCSD (NUYFIZ). The novel compounds **9**–**12** are isostructural, considering the substituted phenanthroline units and/or replacement of the methacrylate ligands by aromatic or aliphatic carboxylic acids.

Given the promising results from the previous section, we applied the design strategy established for the Eu_8Ti_{10}-based POTs to redshift the absorption edge of **8**. Substitution of the phenanthroline ligand at the 5,6- and 4,7-positions leads to the cages $Eu_2Ti_4O_6(Mephen)_2(met)_{10}$ (Mephen = 5,6-dimethyl-1,10-phenanthroline (**9**), $Eu_2Ti_4O_6(OMephen)_2(met)_{10}$ (OMephen = 4,7-dimethoxy-1,10-phenanthroline (**10**) and $Eu_2Ti_4O_6(NH_2phen)_2(met)_{10}$ (NH_2phen = 5,6-diamino-1,10-phenanthroline (**11**). The co-ligand methacrylate present in **8**–**10** was successfully replaced with 4-methoxybenzoate, similar to the work of Zheng et al., giving $Eu_2Ti_4O_6(phen)_2(OMeba)_{10}$ (**12**).[19] The long-chain octanoate ligand was also successfully incorporated to give $Eu_2Ti_4O_6(OMephen)_2(oct)_{10}$ (oct = octanoate, **13**). All the new cages **9**–**13** adopt the same structure as **8**, as revealed by X-ray single-crystal analysis, with the met and/or phen units being replaced by the respective carboxylate and substituted phen ligands.

As with the Eu_8Ti_{10}-based cages described in the previous section, electron-donating substituents in the phen ligands cause a bathochromic shift of the absorption edge in the UV-vis spectra (**Figure 5**). Comparison of the absorption edges of **8**, **9**, **10**, and **11**, all containing methacrylate supporting ligands and phenanthroline ligands with increasing electron-donating character, reveals a systematic increase from ≈300 nm for **8** (phen), to ≈315 nm for **9** (Mephen), ≈350 nm for **10** (OMephen) and ≈400 nm for **11** (NH_2phen). The result is that while **8** and **9** are colorless, **10** is orange-brown and **11** is deep red. The replacement of the met ligands of **8** with electron-donating aromatic OMeba ligands in **12** also results in a red-shift of the absorption edge compared to **8** (to ≈325 nm), whereas the octanoate ligands in compound **13** give a similar result to the analogous methacrylate-substituted cage **10**.

The emission properties of the Eu_2Ti_4-based cages **8**–**13** are presented in Table 2. Compared to the Eu_8Ti_{10}-based benzoate systems **1**–**6** these POTs exhibit significantly higher quantum

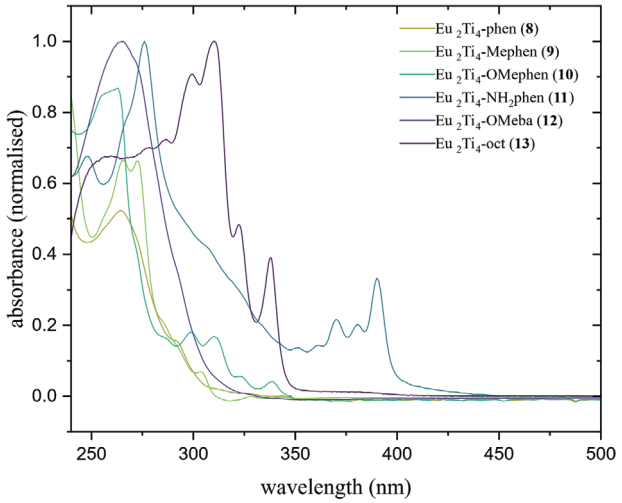

Figure 5. Normalized solution-state UV–vis absorption spectra for the Eu_2Ti_4-based compounds **8**–**13** (0.033 mg mL^{-1} in DCM).

yields, which is due to the more efficient sensitization of the Eu^{3+}-centers caused by both the direct coordination of the light-harvesting antenna ligand to the metal ions and the longer radiative lifetime, indicating a more rigid and shielded Eu^{3+} environment. In compound **11**, however, the emission spectrum shows a large peak ≈400–450 nm, which is attributed to a ligand-centered emission (Figure S7, Supporting Information). This, in combination with a PLQY of only 1%, indicates poor sensitization of the Eu^{3+} ion either due to significant energy back transfer to the ligand or no ET at all due to a mismatching of energy levels (Figure 1b).[20] In general, the ligand T_1 state should lie within a range of 2500–4000 cm^{-1} above the accepting energy levels in Eu^{3+}, from which radiative emission to the ^7F ground states can occur, to allow optimal ET.[21] A more detailed discussion on the T_1-to-Eu^{3+} ET is given in Supporting Information (Figures S8 and S9, Supporting Information).

As a result of the promising optical properties of compounds **10** and **13**, these were incorporated into further test films and analyzed. The long alkyl chains in compound **13** lead to a significant enhancement of its solubility, making it compatible with a variety of commercial polymers (see section 2.3). In general, the absorption and emission properties of these cages were maintained in the films (Figures S5 and S9, Supporting Information). Although PMMA films containing **10** and **13** showed sufficiently high quantum yields, compound **13** was chosen for the subsequent plant growth trials due to its broader compatibility with polymer matrices.

2.3. Large-Scale Film Production

In preparation for growth trials, a procedure for the large-scale synthesis of compound **13** was developed as a first step. The initial synthesis adapted from the literature involved solvothermal conditions, long reaction times (7 days) and a large excess of the high-cost phenanthroline ligand and therefore required optimization.[16] However, using conventional laboratory glassware and refluxing the reaction mixture containing 1.25 equivalents of the phenanthroline ligand under inert conditions for 72 h (as supposed to 11 equivalents in the original work, w.r.t. $Eu(OAc)_3$), highly pure samples of **13** were obtained as indicated by powder diffraction and elemental analysis (yield 75%). All active materials used for the following plant growth trials were synthesized by this method. An alternative for the large-scale synthesis of Eu-containing POTs is the use of a flow reactor. Initial trials were carried out based on the literature synthesis of compound **1**. After optimization of the solvent system (use of hexane as an anti-solvent) compounds **1**–**6** were successfully synthesized in flow in good yields (Scheme S1, Supporting Information). A similar procedure for the synthesis of compound **13** will be targeted in the future.

The thermal stability of **13** was assessed by TGA (Figure S4, Supporting Information). Compared to compound **8**, the decomposition starts significantly earlier (≈205 °C as supposed to 330 °C). The weight loss for both compounds is initiated by a sharp drop to ≈80% of the initial mass, which subsequently flattens out. Due to the reduced thermal stability, any industrial process involving compound **13** could only operate at low temperatures (below 200 °C) to avoid decomposition of the active material.

The incorporation of **13** into plastics started with the fabrication of free-standing, solution-cast PMMA films, shown in **Figure 6**. However, we then took a further step by incorporating **13** into organic- and water-based paints, which can be applied to a variety of surfaces, specifically pre-existing glass greenhouses (**Figure 7**).[22]

The first paint samples applied on borosilicate glass were based on (organically soluble) polypropylene formulations, selected due to commercial availability, optical properties, and cost (Figure 7a). The resulting films showed high light transmission and good emission, but their stability towards light-exposure and atmospheric moisture was low and resulted in quenched luminescence and the paint peeling off the glass after 3–5 weeks. This directed us to the development of water-based paints, which are more environmentally stable. We showed that **13** can be dissolved into (water-based) clear acrylic paint (Figure 7b) and can even be used in conjunction with commercial whitewash (Figure 7c). The acrylic-based formulation gave both sufficiently optically transparent and robust films for plant growth trials.

2.4. Greenhouse Trials

Using the optimized acrylate-based paint, plant growth trials were carried out between June-July 2023. Details of the coating process, its optimization and the characterization of the coatings are given in the Supporting Information (Sections 1.6 and 8, Supporting Information). Eight 1.3 m width x 2.6 m length domestic greenhouses (four coated with active material, four uncoated) were used to grow basil and strawberry plants, crops typically grown under protection (e.g., glasshouses and polytunnels) (**Figure 8**). The eight greenhouses were arranged in four pairs (randomized coated and uncoated), and each house contained ten 500 mL-volume pots of basil plants with six plants each, and 12 strawberry plants transplanted into coir slabs. Basil plants were grown for 5 weeks and then fresh and dry weights of stem and leaf were determined for eight of the ten pots, and leaf numbers and stem lengths were obtained for four of these eight pots. For

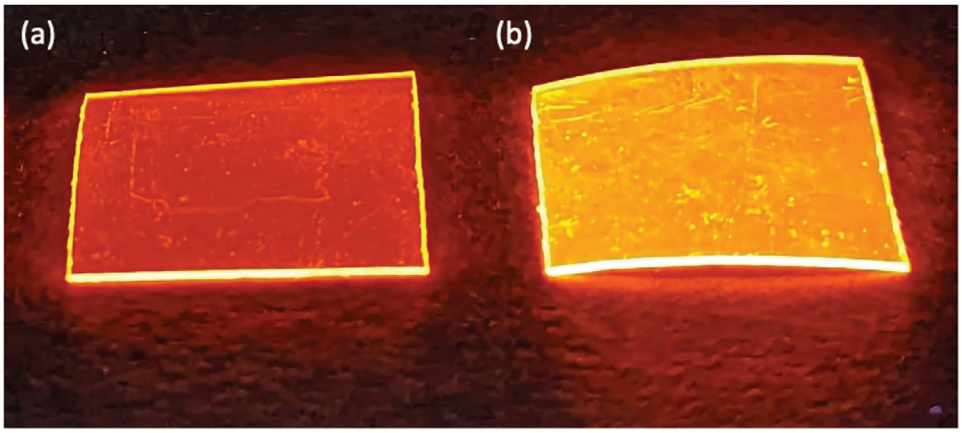

Figure 6. Photographs of PMMA film samples of a) compound **1** and b) compound **13** (5 mg g^{-1}) under 302 nm irradiation. The samples were obtained by solution-casting.

strawberries, the fruit was picked every three days to obtain cumulative fruit yield (fresh weight), and fruit sugars were estimated using a Brix meter at harvest.

For the basil plants, there was an 9.3% increase in leaf dry weight on a per pot basis (g of leaf per pot) in coated versus uncoated greenhouses, indicative of potentially a higher crop yield, but this was not quite significant at the 5% level by one-way ANOVA ($P = 0.063$). From the four pots where leaves were counted, we observed a 9.8% higher leaf dry weight on a per leaf basis (g per leaf) in the coated treatment (highly significant $P < 0.001$ by one-way ANOVA), which would be considered an increase in basil quality (Figure S20, Supporting Information). There was no difference in plant height, but there were 0.5 fewer leaves on average in the coated versus uncoated (10.52 vs 11.02 leaves per plant), resulting in a significant increase in internode length (height/leaf number) in the coated treatment ($P = 0.009$). In summary, for basil, the coated treatment resulted in slightly fewer leaves, but the mean weight of an individual leaf was greater (i.e., fewer, bigger leaves), and the data were suggestive of an overall increase in total leaf biomass, but this was not statistically significant. For strawberry plants, there were no statistically significant or suggestive differences in fruit yield, fruit number, fruit weight (g per fruit) and Brix (P values ranged from 0.23 to 0.68) (Figure S21, Supporting Information). This species-specific effect of the coating is not surprising as physiological responses to light regimes are well known to differ between crops. It is also worthwhile mentioning that our modular approach to LDS molecules, which should allow other lanthanides to be incorporated with different emission wavelengths, provides the means for tailoring the emission properties of the coatings to a specific crop.

The temperature was logged in the greenhouses every 15 min during June and July, and it was clear that the daily mean temperature (mean of all readings within a 24-h period) and the mean maximum daily temperature were lower by 0.5 °C and 3.1 °C, respectively, inside the coated greenhouses (Figure S19, Supporting Information); this reduction in temperature would be expected to be beneficial to crop growth as the summer temperatures were above optimum (mean maximum temperature in uncoated was 37.2 °C).

The glass panels were shown to emit PAR when illuminated by UV-B light (302/312 nm; Figure S15, Supporting Information), but at a low level (up to 4 µmol m^{-2} s^{-1}, measured by SunScan Canopy Analysis System, Delta T Devices, Cambridge, UK; data not shown) relative to typical light intensities on a bright summer day in the UK (up to 1400 µmol m^{-2} s^{-1}, Figure S22a,b, Supporting Information). Therefore, we tested whether the coated glass was able to enhance the PAR experienced by the plants growing under ambient sunlight, taking measurements with the SunScan Canopy Analysis System. PAR readings were taken in each of the eight greenhouses once a week in June 2023 with the 1 m long SunScan probe placed inside each greenhouse at plant height (Figure S22a, Supporting Information). Across the four weeks, the mean percentage difference in PAR (± standard deviation) was 7.7 ± 1.2% lower inside the coated greenhouses compared to the uncoated ones ($P = 0.013$; paired two sample t-test), presumably due to reduced total light transmission through the coating (Figure S17, Supporting Information).

Figure 7. Photographs of the development of the paint samples using compound **13** on borosilicate glass with a) polypropylene-based paint, b) acrylic-based paint, and c) in commercial whitewash (left – ambient light; right – under UV). All samples are under 302 nm UV light.

Figure 8. a) The randomized block design of the trial greenhouses. b) Growth layout for strawberries and c) basil plants. In each greenhouse there were 12 strawberry plants grown in two coir slabs automatically fed with Vitax 2-1-4 (Vitax Ltd, Coalville, UK), and ten pots containing six basil plants growing in All Purpose peat-based compost (Sinclair, Ellesmere Port, UK) with automatic irrigation.

In addition, we utilized a sensor (BF5 Sunshine Sensor, DeltaT, Cambridge, UK) equipped with a photodiode array and a shading pattern to detect the total and diffuse component of PAR (Figure S22b, Supporting Information). Data were collected inside each greenhouse (n = 4 replicates) with the sensor mounted on a tripod and levelled at plant height; treatments were compared with a students t-test (two samples, assuming equal variances and two-tailed *P* values). The coating reduced the mean total PAR by 14.1% from 1351±54 to 1161±67 μmol m^{-2} s^{-1} (P = 0.005), but increased the diffuse component from 376±65 to 476±29 μmol m^{-2} s^{-1} (an increase of 26.5%; P = 0.031).

Overall, a positive impact on the growth behavior of the basil plants was observed. However, given the measured reduction of PAR inside the coated greenhouses, this enhancement is most likely caused by the increase in scattered light or reduction of sub-optimal temperatures through shading, rather than the down-shifting effect of the active material. To quantify the effect of the acrylic paint alone on the growth of the plants an additional set of greenhouses coated with only acrylic paint (no emissive material) will be included in future plant growth trials. In a similar previously published study on down-shifting coatings for greenhouses the scattering effect of the paint material alone was not investigated, which, in combination with the absence of PAR measurements puts the origin of the observed increase in plant growth into question.[14]

3. Conclusion

In this work, a series of Eu-containing POTs was synthesized and analyzed in order to assess their suitability as LDS materials for plant growth enhancement. Starting from an Eu_8Ti_{10}-based POT system the effect of a modification of the ligand periphery on the optical properties of the compounds was investigated. The introduction of electron-donating substituents like OMe-groups was shown to successfully shift the absorption edge of the compound, allowing for a larger part of the solar spectrum to be converted to red light (600–700 nm). The use of a more efficient sensitizing antenna ligand in the Eu_2Ti_4-based POTs was found to improve the efficiency of the emission process (PLQY). Some insight in the intramolecular ET processes was obtained through low-temperature spectra showing a ligand triplet state matching the energy of the $^5D_2$- and $^5D_0$-levels in Eu^{3+} for sensitization. The optimized Eu-POT was successfully incorporated in a variety of polymer films and acrylic paints whilst maintaining its optical properties. The systematic, modular approach to the development of LDS materials which we have developed here provides the first sprayable coatings of this type, applicable to a real agricultural environment and the means by which the specific light requirements of crops might be tailored by the incorporation of POTs containing different lanthanides or mixtures of lanthanides.

In a greenhouse trial, the impact of the down-shifting material on the growth of basil and strawberry plants was investigated. Although an increase in leaf dry weight was observed for the basil plants grown in coated greenhouses, this improvement can most likely be assigned to the increase in scattered light caused by the coating itself, as a simultaneous reduction of the PAR inside the coated greenhouses was also observed. Further improvement of the transmission of the coating is therefore required for the LDS material to have a measurable impact on the plant growth under real-world conditions.

In addition to a coating-only control greenhouse (without emissive material) to quantify the impact of the coating itself on the outcome of the trials, a new series of trials will

investigate plant-specific effects of coatings on growth. While this sprayable technology is a significant advance in this area, there are some obvious challenges ahead. Specifically, one of the keys to improving the performance of the LDS materials for future commercial applications will be to increase their light-harvesting ability by broadening the range of absorption from the UV alone (only 3% of ambient light) into the visible spectrum, in order to increase the total photon flux for down-shifting. This in turn will increase the total number of photons transferred by LDS for plant growth. Since the absorption characteristics of the LDS materials are governed by the antenna ligand used, employing antenna ligands with absorption >400 nm will be the next development in this area, using the modular design approach which we have established in this work.

Supporting Information

Supporting Information is available from the Wiley Online Library or from the author.

Acknowledgements

R.M. and B.O-E. contributed equally to this work. R.M. would like to thank the Todd-Hamied fund (Cambridge) and the Cusanuswerk e.V. for financial support. Lambda Energy would like to acknowledge Innovate UK and the Department of Net Zero for the Energy Entrepreneurs Fund 8 and 9 grants that have funded the materials and labour costs. Both KIT and Lambda Energy would like to acknowledge funding from PhotonHub (project P2022-35), while KIT is also grateful to financial support from the Helmholtz Association – Materials and Technologies for the Energy Transition (MTET) – Topic 1 Photovoltaics (38.01.05). Plant growth trails were supported by the Technology Accelerator Fund at Cranfield, enabled by Green Future Investments Ltd. R.M. and B.O-E. are joint first author of the paper. R.M. developed the fundamental concepts behind in this work, as well as synthesized and characterized all novel compounds under the supervision of D.S.W. B.O-E. developed the synthesis of compounds **1**–**6** in flow and characterized the materials developed in flow under the supervision of P.C. N.J.J. developed and optimized the large-scale synthesis of compound **13** and developed the paints for the coating of greenhouse panels under B.B supervision. B.B. developed the polymer films used for PLQY measurements. A.D.B. and G.K.K carried out all single-crystal X-ray crystallography. L.M.B.C., D.G., T.W.W., I.G.T., E.G. and A.J.T. undertook the plant growth trials. D.B., I.A.H., and B.S.R. carried out the luminescence measurements (PLQYs, low-temperature spectra) and analyzed the data. M.S.S. was an industrial supervisor. All collaborators contributed to the modular design, discussed the material properties and facilitated the development of further generations in frequent meetings as supervised by N.J.J, B.B. and M.S.S.

Conflict of Interest

Authors N.J.J., M.S.S., and B.B. were employed by Lambda Energy, Ltd. while conducting these experiments and may also have equity in the company.

Data Availability Statement

The data that support the findings of this study are available in the supplementary material of this article.

Keywords

down-shifting, food security, plant growth, polyoxotitanates

Received: June 26, 2024
Revised: October 21, 2024
Published online:

[1] Framework Convention on Climate Change, http://unfccc.int/resource/docs/2015/cop21/eng/l09.pdf, (accessed: March, 2024).
[2] United Nations, World Population Prospects 2022, https://population.un.org/wpp/Graphs/Probabilistic/POP/TOT/900, (accessed: March, 2024).
[3] M. Mykhailova, O. Yatsenko, Y. Zavadska, O. Afanasieva, R. Haas, *Die Bodenkultur: J. Landmanage., Food Environ.* **2023**, *74*, 91.
[4] S. Sanford, Reducing greenhouse energy consumption – An overview, https://farm-energy.extension.org/wp-content/uploads/2019/04/2.-A3907-01.pdf, (accessed: March, 2024).
[5] K. Harbick, L. D. Albright, *Acta Hortic.* **2016**, *1134*, 285.
[6] B.-S. Wu, A.-S. Rufyikiri, V. Orsat, M. G. Lefsrud, *Plant Sci.* **2019**, *289*, 110272.
[7] P. Kusuma, P. M. Pattison, B. Bugbee, *Hortic. Res.* **2020**, *7*, 56.
[8] M. Plouzeau, S. Piogé, F. Peilleron, L. Fontaine, S. Pascual, *J. Appl. Polym. Sci.* **2022**, *139*, e52861.
[9] G. Seybold, G. Wagenblast, *Dyes Pigm.* **1989**, 11.
[10] a) D. Hebert, J. Boonekamp, C. H. Parrish, K. Ramasamy, N. S. Makarov, C. Castañeda, L. Schuddebeurs, H. McDaniel, M. R. Bergren, *Front. Chem.* **2022**, *10*, 1; b) C. H. Parrish, D. Hebert, A. Jackson, K. Ramasamy, H. McDaniel, G. A. Giacomelli, M. R. Bergren, *Commun. Biol.* **2021**, *4*, 124.
[11] Z. Xu, M. Michalska, I. Papakonstantinou, *ACS Appl. Mater. Interfaces* **2024**, *16*, 27587.
[12] J. Jean, J. Xiao, R. Nick, N. Moody, M. Nasilowski, M. Bawendi, V. Bulovic, *Energy Environ. Sci.* **2018**, *11*, 2295.
[13] a) ENGINEERING SUNLIGHT FOR INCREASED PRODUCTIVITY, http://LLEAF.com, (accessed: March 2024); b) http://www.lightcascade/com/en/technology/, (accessed: March 2024).
[14] S. Shoji, H. Saito, Y. Jitsuyama, K. Tomita, Q. Haoyang, Y. Sakurai, Y. Okazaki, K. Aikawa, Y. Konishi, K. Sasaki, K. Fushimi, Y. Kitagawa, T. Suzuki, Y. Hasegawa, *Sci. Rep.* **2022**, *12*, 17155.
[15] D.-F. Lu, Z.-F. Hong, J. Xie, X.-J. Kong, L.-S. Long, L.-S. Zheng, *Inorg. Chem.* **2017**, *56*, 12186.
[16] Compound 7 was only characterized via single-crystal XRD and not isolated as bulk material.
[17] M. H. Werts, R. T. Jukes, J. W. Verhoeven, *Phys. Chem. Chem. Phys.* **2002**, *4*, 1542.
[18] X.-P. Shu, W. Luo, H.-Y. Wang, M.-Y. Fu, Q.-Y. Zhu, J. Dai, *Inorg. Chem.* **2020**, *59*, 10422.
[19] Y. Deng, X. Zheng, H. Zheng, H. Xu, F. Li, L. Long, L. Zheng, *Sci. China Mater.* **2021**, *64*, 2883.
[20] M. Osawa, M. Hoshino, T. Wada, F. Hayashi, S. Osanai, *J. Phys. Chem. A* **2009**, *113*, 10895.
[21] M. Latva, H. Takalo, V.-M. Mukkala, C. Matachescu, J. C. Rodriguez-Ubis, J. Kankare, *J. Lumin.* **1997**, *75*, 149.
[22] It can be noted in this regard that the previous report of the use of a dichloromethane paint of $[Eu(hfa)_3(TPPO)_2]$ onto polyolefin sheets would not be applicable to glass and its toxicity makes it unsuitable for an agricultural setting.
[23] a) F. L. K. Kempkes, C. Stanghellini, N. Garcia Victoria, M. A. Bruins, *Acta Hortic.* **2012**, *952*, 255; b) T. Dueck, J. Janse, T. Li, F. Kempkes, B. Eveleens, *Acta Hortic.* **2012**, *956*, 75.